A New Predictive Lateral Load Transfer Ratio for Rollover Prevention Systems

Chad Larish, Damrongrit Piyabongkarn, Vasilios Tsourapas, and Rajesh Rajamani

***Abstract*—In rollover prevention systems, a real-time lateral load transfer ratio (LTR) is typically computed to predict the likelihood of a vehicle to rollover and, hence, initiate rollover prevention measures. A traditional LTR largely relies on a lateral accelerometer signal to calculate rollover propensity. A new predictive LTR (PLTR) is developed in this paper, which utilizes a driver's steering input and several other sensor signals available from the vehicle's electronic stability control system. The new PLTR index can provide a time-advanced measure of rollover propensity and, therefore, offers significant benefits for closed-loop rollover prevention. Simulation results are presented using the industry-standard software CarSim to demonstrate the benefits of the new PLTR index. Experimental results of open-loop comparisons between LTR and PLTR indexes are presented, followed by experimental results on the closed-loop implementation of a PLTR-based rollover prevention system. The results in this paper document how a predictive rollover index can be developed and the advantages of such a system in rollover prevention.**

***Index Terms*—Active vehicle safety, rollover detection, rollover prevention, vehicle dynamics.**

NOMENCLATURE

a	Longitudinal distance from the center of gravity (CG) to the front axle.
A_y	Vehicle lateral acceleration.
A_{y_meas}	Measured vehicle lateral acceleration.
b	Longitudinal distance from the CG to the rear axle.
C_f	Front-tire cornering stiffness.
C_r	Rear-tire cornering stiffness.
d	Track width.
$F_{x\mathrm{fl}}$	Front-left-tire longitudinal force.
$F_{x\mathrm{fr}}$	Front-right-tire longitudinal force.
$F_{x\mathrm{rl}}$	Rear-left-tire longitudinal force.
$F_{x\mathrm{rr}}$	Rear-right-tire longitudinal force.
$F_{y\mathrm{fl}}$	Front-left-tire lateral force.
$F_{y\mathrm{fr}}$	Front-right-tire lateral force.
$F_{y\mathrm{rl}}$	Rear-left-tire lateral force.
$F_{y\mathrm{rr}}$	Rear-right-tire lateral force.
g	Gravity acceleration.
h	Distance from sprung mass CG to roll center.
h_R	Roll center height.
$I_{xx,yy,zz}$	Moment of inertia about respective axes.
m	Vehicle sprung mass.
r	Yaw rate.
u	Vehicle's longitudinal velocity.
v	Vehicle's lateral velocity.
β	Vehicle body slip angle.
δ	Steering-wheel angle.
ϕ_r	Road bank angle.
ϕ_v	Vehicle roll angle.

Manuscript received March 27, 2012; revised August 13, 2012 and January 9, 2013; accepted January 27, 2013. Date of publication March 15, 2013; date of current version September 11, 2013. The review of this paper was coordinated by Prof. T. Shim.

C. Larish, D. Piyabongkarn, and V. Tsourapas are with Eaton Corporation, Innovation Center, Eden Prairie, MN 55344 USA (e-mail: ChadLarish@eaton.com; NengPiyabongkarn@eaton.com; VasiliosTsourapas@eaton.com).

R. Rajamani is with the University of Minnesota, Minneapolis, MN 55455 USA (e-mail: rajamani@me.umn.edu).

Color versions of one or more of the figures in this paper are available online at http://ieeexplore.ieee.org.

Digital Object Identifier 10.1109/TVT.2013.2252930

I. INTRODUCTION

VEHICLE rollover has been identified as the vehicle crash type with the highest fatality. According to the National Highway Traffic Safety Administration (NHTSA) [1], vehicle rollovers account for approximately 3% of passenger-vehicle crashes annually. However, 33% of fatalities involved with all passenger-vehicle crashes are related to rollover accidents. Continued popularity of high-CG vehicles, such as SUVs and trucks, lends reason to further development of anti-rollover systems as these types of vehicles are most often associated with incidents involving vehicle rollover.

Rollover detection and prevention have been studied by many researchers [2]–[7], [11], [12], [14]. Several different means of detecting vehicle rollover have been introduced, such as the lateral load transfer ratio (LTR) and the time-to-rollover metric [8]–[10], [14]. The latter method needs precise vehicle model parameters to be able to predict the vehicle roll angle ahead of time. The LTR defines vehicle rollover as the moment when either the left or the right wheel of the vehicle experiences lift-off from the ground. This index only gives a snapshot of vehicle dynamics by detecting instantaneous load transfer due to lateral acceleration, regardless of the overall steering pattern. Analytical calculations and experimental data are used to define a threshold for determining rollover threat based on estimated values of the LTR. If the threshold is set too low, the LTR will provide a warning or activate the rollover prevention system even during safe normal driving. If the threshold is set too high, a preventive action may activate too late to avoid vehicle rollover. Identifying a good LTR threshold is difficult because of dynamic changes and unexpected disturbances, which cannot be captured using only a lateral-acceleration-based LTR.

This paper proposes a new predictive LTR (PLTR). This predictive index is based on factors that occur over a time horizon. It will indicate future vehicle rollover propensity based on both the current LTR and the driver's steering angle input.

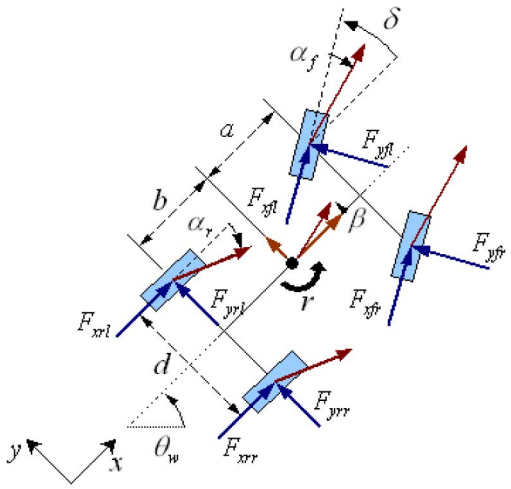

Fig. 1. Vehicle lateral dynamics.

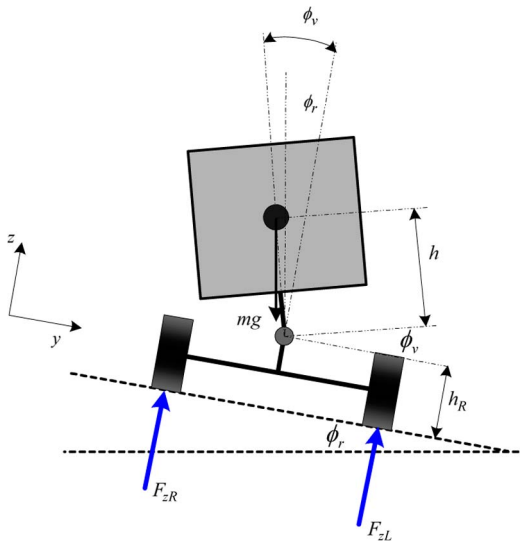

Fig. 2. Vehicle roll dynamics.

The decision to use the steering-wheel angle as a means of prediction in the PLTR can further be supported by the findings in [9], which concluded that the factors associated with steering had the greatest capability of providing the earliest rollover warning.

The outline of this paper is as follows. First, the LTR, which is an index based on a half-car vehicle dynamic model and on the use of sensors to detect lateral acceleration, yaw rate, and sprung mass roll angle, will be presented. Simulations conducted in CarSim on various car types to better define the precision and accuracy of a modified LTR index follow. Validation with experimental data is also provided. Further estimation of the new LTR based solely on the body-fixed lateral acceleration of the vehicle is also discussed. Then, the new predictive rollover index, i.e., PLTR, is derived. The derivation of the PLTR is followed by simulation results that conclusively show the effectiveness of this new index in predicting impending rollover. Finally, the effectiveness of anti-rollover control is presented using the PLTR and LTR indexes that are experimentally implemented on a vehicle equipped with actively controlled electrohydraulic limited-slip differentials.

II. Vehicle Model

The variables used for this vehicle model are defined in the Nomenclature. Fig. 1 shows the lateral dynamics of the vehicle. The vehicle yaw angle direction and instantaneous yaw rate, velocity, and slip angles are also indicated in this diagram. Fig. 2 shows the roll dynamics of the vehicle. The effect of the vehicle's unsprung mass on roll dynamics is neglected. Distances associated with the roll center location and the vehicle roll angle and the road bank angle are also specified in the figure.

The vehicle lateral dynamics can be written as

$$\begin{aligned}\sum F_y &= mA_y = F_{y\mathrm{rl}} + F_{y\mathrm{rr}} + (F_{y\mathrm{fl}} + F_{y\mathrm{fr}}) \\ &\quad \cdot \cos\delta + (F_{x\mathrm{fl}} + F_{x\mathrm{fr}}) \cdot \sin\delta \qquad (1)\end{aligned}$$

$$\begin{aligned}&(I_{xx} + mh^2) \cdot (\ddot{\phi}_v - \ddot{\phi}_r) \\ &\quad = (F_{zL} - F_{zR}) \cdot \frac{d}{2} + \sum F_y \cdot h \cdot \cos\phi_v \\ &\qquad + mgh \cdot \sin\phi_v \cdot \cos\phi_r - mgh \cdot \cos\phi_v \\ &\qquad \cdot \sin\phi_r + \left[(I_{yy} - I_{zz}) - mh^2\right] \cdot r^2 \\ &\qquad \cdot \sin(\phi_v - \phi_r)\cos(\phi_v - \phi_r) \qquad (2)\end{aligned}$$

where

$$A_y = \dot{v} + ru - g \cdot \sin\phi_r + hr^2 \cdot \sin\phi_v + h\dot{\phi}_v^2 \cdot \sin\phi_v - h\ddot{\phi}_v \cdot \cos\phi_v.$$

The vertical dynamics of the sprung mass can be expressed as

$$\begin{aligned}m\ddot{z} &= m \cdot \left(\dot{\phi}_v^2 h \cdot \cos\phi_v + \ddot{\phi}_v h \sin\phi_v\right) \\ &= (F_{zL} + F_{zR}) - mg \cdot \cos\phi_r. \qquad (3)\end{aligned}$$

If the bank angle is zero, the equations can be written as follows:

$$\begin{aligned}&\sum F_y \\ &\quad = m \cdot \left(\dot{v} + ru + hr^2 \cdot \sin\phi_v + h\dot{\phi}_v^2\right. \\ &\qquad \left. \cdot \sin\phi_v - h\ddot{\phi}_v \cdot \cos\phi_v\right) \qquad (4)\end{aligned}$$

$$\begin{aligned}&(I_{xx} + mh^2) \cdot \ddot{\phi}_v \\ &\quad = (F_{zL} - F_{zR}) \cdot \frac{d}{2} + \sum F_y \cdot h \cdot \cos\phi_v + mgh \cdot \sin\phi_v \\ &\qquad + \left[(I_{yy} - I_{zz}) - mh^2\right] \cdot r^2 \cdot \sin\phi_v \cdot \cos\phi_v \qquad (5)\end{aligned}$$

$$\begin{aligned}m\ddot{z} &= m \cdot \left(\dot{\phi}_v^2 h \cdot \cos\phi_v + \ddot{\phi}_v h \sin\phi_v\right) \\ &= (F_{zL} + F_{zR}) - mg. \qquad (6)\end{aligned}$$

TABLE I
SIMULATION VEHICLE PARTICULATES

Quantity	Symbol	Value	Unit
Mass	m	4400	Kg
C.G. Height	h	0.94	m
Track width	d	1.819	m

III. LATERAL LOAD TRANSFER RATIO

A common index that is used to quantify vehicle rollover propensity is the lateral transfer ratio (LTR), which is defined as

$$\text{LTR} := \frac{F_{zR} - F_{zL}}{F_{zL} + F_{zR}}. \tag{7}$$

This index utilizes left and right vertical tire forces F_{zL} and F_{zR}. The LTR defines vehicle rollover initiation as the moment when either the left or the right side of the vehicle experiences lift-off from the ground. The LTR varies from -1 to 1, where -1 and 1 refer to either the right or the left vehicle tire losing contact with the ground, respectively. An LTR value of 0 refers to equal vertical forces on both sides of the vehicle (zero roll). This index, similar to most currently studied indexes, only considers a snapshot of vehicle dynamics, such as the dominant lateral acceleration trait at that time instant, regardless of the overall steering pattern. Through the use of this index, the time between detection of potential rollover characteristics and the moment rollover occurs may sometimes be too small for a rollover prevention system to stop the vehicle from rolling over.

Utilizing (5) and (6) to calculate $F_{zR} - F_{zL}$ and $F_{zR} + F_{zL}$, assuming that $\dot{\phi}_v$ and $\dot{\phi}_v$ are zero and substituting into (7), the following expression is obtained:

$$\text{LTR} = \frac{2}{d} \cdot \frac{h \cdot \left(\cos\phi_v \cdot (\dot{v} + ru) + hr^2 \cdot \sin\phi_v + g \cdot \sin\phi_v\right)}{g}. \tag{8}$$

Using assumptions $\cos^2\phi_v \approx 1$, $hr^2 \approx 0$, and $\dot{v} + ru = A_{y\_\text{meas}} \cdot \cos\phi_v$, the final expression of the estimated LTR is obtained as

$$LTR_e = \frac{2h}{dg}[A_{y\_\text{meas}} + g \cdot \sin\phi_v] \tag{9}$$

where A_{y_meas} is the measured lateral acceleration of the vehicle. To validate the given expression for an estimate of the LTR, the CarSim simulation tool is utilized. CarSim is an industry-standard vehicle simulation software containing a full dynamic model of a vehicle with many degrees of freedom. The simulated vehicle is a large SUV with parameters given in Table I.

Note that the height of the CG was increased from the standard 0.83 m to simulate a top-loaded vehicle state that results in a rollover scenario during an NHTSA fishhook maneuver. Furthermore, the vehicle is simulated with open differentials and no active rollover mitigation properties. Figs. 3 and 4 show the simulation results comparing the actual LTR [see (7)] and the estimated LTR [see (8)] during a double-lane change and an NHTSA fishhook maneuver, respectively. Very good matching is observed between the actual and the estimated LTR in both the NHTSA fishhook and double-lane change maneuvers. Specifically for the NHTSA fishhook, wheel lift-off occurs at t = 2.8 s, and the LTR is well estimated up to that point; after wheel lift-off occurs, the actual LTR stays at the value of 1 since the tire vertical forces on one side become 0.

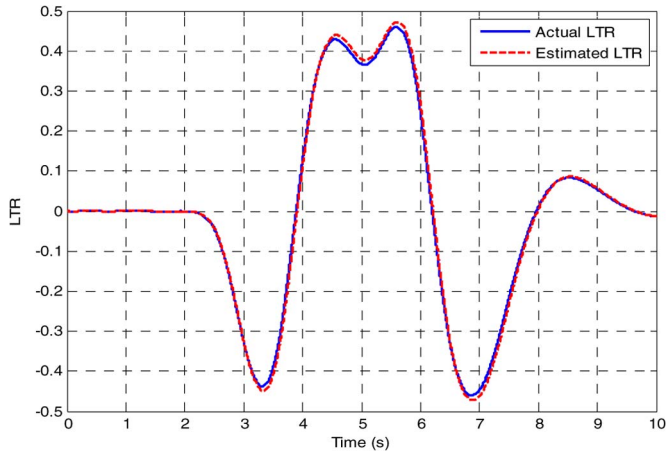

Fig. 3. Actual versus estimated LTR during a double-lane change maneuver at 80 km/h.

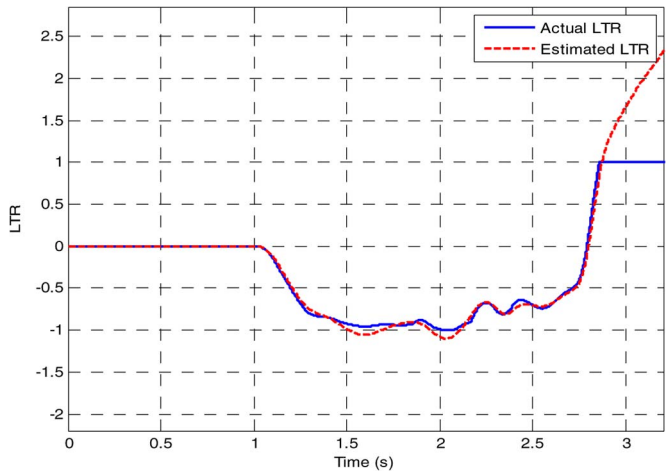

Fig. 4. Actual versus estimated LTR during a fishhook maneuver at 70 km/h.

IV. PREDICTIVE LOAD TRANSFER RATIO

A typical LTR is estimated from instantaneous measurements obtained at a given time. Information gathered at a fixed time is used to determine immediate, as opposed to future, rollover threat. Analytical calculations and experimental data contribute to the choice of a threshold for determining rollover threat based on estimated values of the LTR. If the threshold is set too low, the LTR will give a warning or activate the rollover prevention system even for normal safe driving. If the threshold is set too high, a preventive action may activate too late to avoid the vehicle from rolling over. Identifying a good LTR threshold is difficult because of dynamic changes and unexpected disturbances, which cannot be captured using only a static LTR.

Hence, a new predictive rollover index, i.e., PLTR, is developed. This predictive index will indicate future vehicle rollover propensity for a wide range of vehicle maneuvers, based on

data collected in the current time frame. The PLTR is defined as follows:

$$\text{PLTR}_{t_0}(\Delta t) = \text{LTR}(t_0) + \dot{\text{LTR}}(t_0) \cdot \Delta t \tag{10}$$

where Δt is the preview time, and t_0 is the current time.

Considering the LTR from (9), it can be further simplified for use in this PLTR derivation as

$$\text{LTR} = \frac{2h}{d}\left[\frac{A_y}{g} + \sin\phi\right]. \tag{11}$$

Hence, we have

$$\text{PLTR}_{t_0}(\Delta t) = \text{LTR}(t_0) + \frac{2h}{d} \cdot \frac{d}{dt}\left[\frac{A_y}{g} + \sin\phi\right] \cdot \Delta t \tag{12}$$

or

$$\text{PLTR}_{t_0}(\Delta t) = \text{LTR}(t_0) + \frac{2h}{d \cdot g} \cdot [\dot{A}_y + g\dot{\phi}]\Delta t. \tag{13}$$

Equation (13) shows the calculation of the PLTR at time t_0 that is predicted for a future time horizon Δt. A_{y_meas} is typically noisy, and it is difficult to obtain a smooth value of its derivative. A filtering technique is first used to address this problem, as shown in the following equation:

$$\text{PLTR}_{t_0}(\Delta t) = \frac{2h}{d}\left[\frac{A_{y\_\text{meas}}}{g} + \sin\phi_{\text{meas}}\right] + \frac{2h}{d \cdot g} \times \left(\frac{s}{\tau s + 1}A_{y\_\text{meas}} + \frac{\tau s}{\tau s + 1}\dot{A}_{y\_\text{meas}} + g\dot{\phi}_{\text{meas}}\right) \cdot \Delta t \tag{14}$$

where τ is a time constant.

The lateral acceleration derivative in the second term can be further estimated from the lateral dynamics (1).

By utilizing a linear approximation and the small angle assumption, the lateral dynamics equation can be written as [13], [14]

$$mA_y = -C_0\beta - C_1\frac{r}{u} + 2C_f\delta \tag{15}$$

where $C_0 = 2C_f + 2C_r$ and $C_1 = 2aC_f - 2bC_r$. C_f and C_r are the cornering stiffness values for the front and rear tires, respectively.

The derivative of (15) can be written as

$$\dot{A}_y = \frac{-C_0(A_y - ru) - C_1\dot{r}}{mu} + \frac{2C_f}{m}\frac{1}{\tau_{\text{sw}}s + 1} \cdot \frac{1}{SR}\dot{\delta}_d \tag{16}$$

where $(\delta_w/\delta_d) = (1/SR) \cdot (1/\tau_{\text{sw}}s + 1)$, δ_d is the driver's steering-wheel angle, τ_{sw} is the steering first-order time constant, and SR is the steering ratio.

By using this model-based filter, the noise from the differentiation of the steering-wheel angle can be filtered out using a low-pass filter. Moreover, the driver's steering input information plays an important role in predicting the rollover index due to the inherent time delay between the steering input and its influence on vehicle roll.

The new PLTR is displayed as follows:

$$\begin{aligned}\text{PLTR}_{t_0}(\Delta t) &= \frac{2h}{d}\left[\frac{A_{y\_\text{meas}}(t_0)}{g} + \sin\phi_{\text{meas}}\right] \\ &\quad + \frac{2h}{d \cdot g}\left\{\frac{s}{\tau s + 1}A_{y\_\text{meas}}(t_0) + \frac{\tau s}{\tau s + 1} \cdot \frac{-C_0(A_y - ru) - C_1\dot{r}}{mu} + \cdots \right. \\ &\quad \left. \cdots + \frac{\tau s}{\tau s + 1} \cdot \frac{2C_f}{m}\frac{s}{\tau_{\text{sw}}s + 1} \cdot \frac{1}{SR}\delta_d(t_0) + g\dot{\phi}_{\text{meas}}\right\} \cdot \Delta t.\end{aligned} \tag{17}$$

Filter $\tau s^2/((\tau s + 1)(\tau_{\text{sw}}s + 1))$ is used on the driver's steering angle. Prediction time Δt needs to be selected to be long enough to cover the rollover prevention system response time.

The term $\sin(\phi_{\text{meas}})$ is approximately proportional to lateral acceleration, as described in [14]. Hence, $\sin(\phi_{\text{meas}})$ can be replaced by kA_{y_meas}. The value of constant k depends on the CG height and suspension parameters and will have to be accordingly tuned for each vehicle. For small roll angles, the term can be entirely ignored. Finally, the final form of the new PLTR is shown as follows:

$$\begin{aligned}\text{PLTR}_{t_0}(\Delta t) &= \frac{2h}{d \cdot g}(1 + kg)A_{y\_\text{meas}}(t_0) \\ &\quad + \frac{2h}{d \cdot g}\left\{\frac{s}{\tau s + 1}A_{y\_\text{meas}}(t_0) + \frac{\tau s}{\tau s + 1} \cdot \frac{-C_0(A_y - ru) - C_1\dot{r}}{mu} + \cdots + \frac{\tau s}{\tau s + 1} \right. \\ &\quad \left. \cdot \frac{2C_f}{m}\frac{s}{\tau_{\text{sw}}s + 1} \cdot \frac{1}{SR}\delta_d(t_0) + g\dot{\phi}_{\text{meas}}\right\} \cdot \Delta t.\end{aligned} \tag{18}$$

This new rollover index has the following advantages over the typical LTR.

1) It acts as part of a warning system to predict rather than detect vehicle rollover.
2) It is easier to set the activation threshold, since the trade-off between false alarms and safety is reduced, due to increased time available for a rollover prevention action.
3) More vehicle information (steering angle, yaw rate, and roll rate) is used in the index. At the same time, all of the required feedback variables can be easily measured with inexpensive sensors available in electronic stability control (ESC) systems.
4) It can be used in rollover prevention systems that include both torque management or brake-based stability control systems and suspension control or other rollover prevention systems.

It should be noted that CG height h plays a prominent role in the computed value of the PLTR. This is no different from the

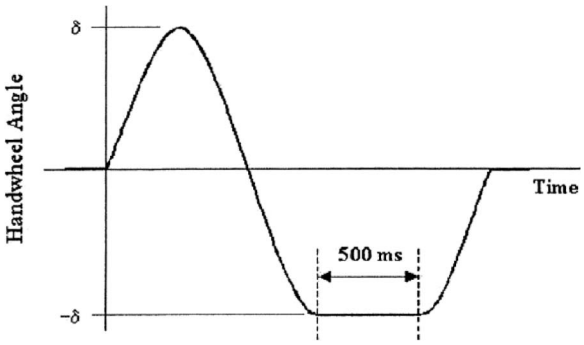

Fig. 5. NHTSA "Sine with Dwell" stability test steering angle.

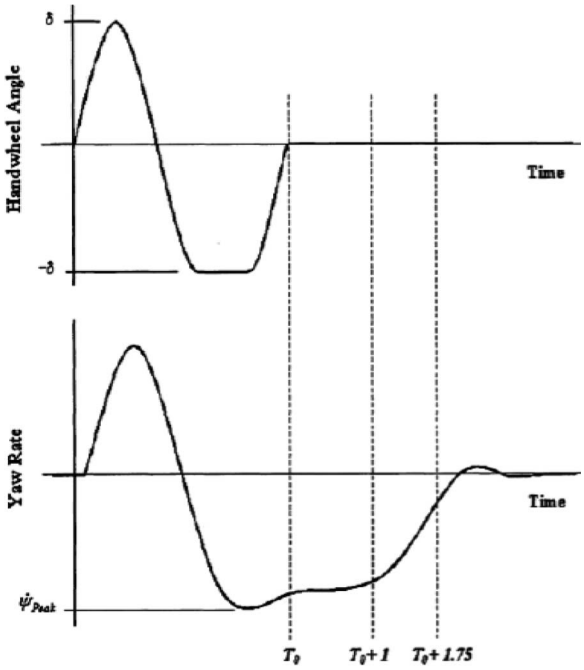

Fig. 6. "Sine with Dwell" failure criteria.

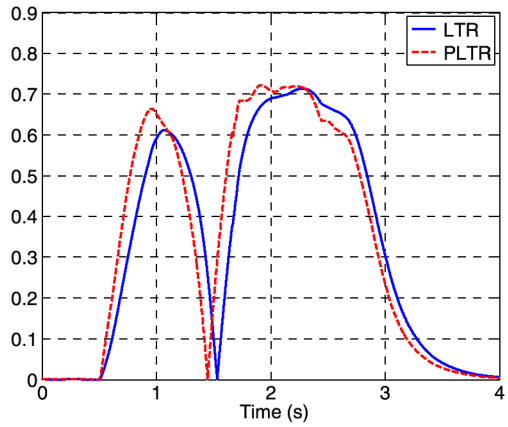

Fig. 7. "Sine with Dwell" at a steering amplitude of 113.8° (simulation).

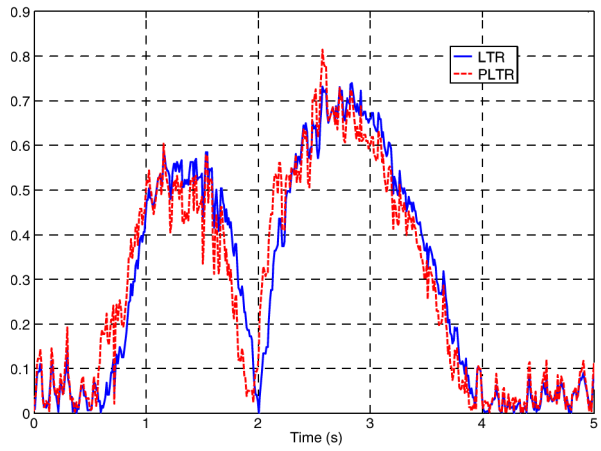

Fig. 8. "Sine with Dwell" at a steering amplitude of 113.8° (experimental measurements).

case of the LTR wherein the CG height value plays an equally prominent role. The real-time estimation of CG height has been addressed by several authors in the literature [11], [14].

The value of tire cornering stiffness also plays a role in the calculation of the PLTR. The value of the cornering stiffness is chosen based on nominal dry-road conditions. The value of cornering stiffness may change when the road becomes icy or slippery. However, an aggressive maneuver on an icy road is less likely to cause rollover than on a dry road. Furthermore, this is not likely to result in false alarms, since the vehicle is more likely to understeer and, the measured angular acceleration and yaw rate are consequently likely to be small on a slippery road. These factors would reduce the real-time value of the computed PLTR and prevent false alarms.

A simulation study utilizing NHTSA's "Sine with Dwell" maneuver (FMVSS 126) [1] was performed to confirm the effectiveness of the PLTR. The NHTSA established the "Sine with Dwell" test to evaluate the effectiveness of all ESC systems as they become standard equipment on all vehicles that are 4536 kg (10 000 lbs) or less in 2012.

The FMVSS 126 standard procedure requires two test maneuvers to complete. The initial test is referred to as "Swept Steer," and the results determine the initial steering angle for the actual "Sine with Dwell" portion of the standard. For the "Sine with Dwell" maneuver itself, the vehicle is given the steering input shown in Fig. 5 while traveling at a speed of 80 km/h ± 2 km/h. The steering pattern is made up of a 0.7-Hz frequency sine wave with a 500-ms delay beginning at the second peak amplitude. The first "Sine with Dwell" run is completed with a sine amplitude of 1.5× the steering angle established with previous "Swept Steer" tests. The amplitude is then increased for each run by an increment of 50% of the initial amplitude.

The successful completion of the "Sine with Dwell" test is primarily determined from vehicle yaw rate at two points during the maneuver. As shown in Fig. 6, the criteria to satisfy the test are the yaw rates of the vehicle at 1 s $(\boldsymbol{T_0 + 1})$ and at 1.75 s $(\boldsymbol{T_0 + 1.75})$ after the time when the steering ceases $(\boldsymbol{T_0})$. These yaw rates have to be less than 35% and 20% of the peak yaw rate $(\boldsymbol{\Psi_{Peak}})$, respectively.

The simulation was performed using a stock Humvee vehicle model to illustrate the effectiveness of the PLTR with 0.3-s predictive time. Fig. 7 shows how the PLTR matches the actual LTR profile and the predictive quality of the PLTR. It is shown that the PLTR shows a time advance (of the order of 100 ms) compared with the LTR. Otherwise, the PLTR roughly matches the shape of the LTR trajectory.

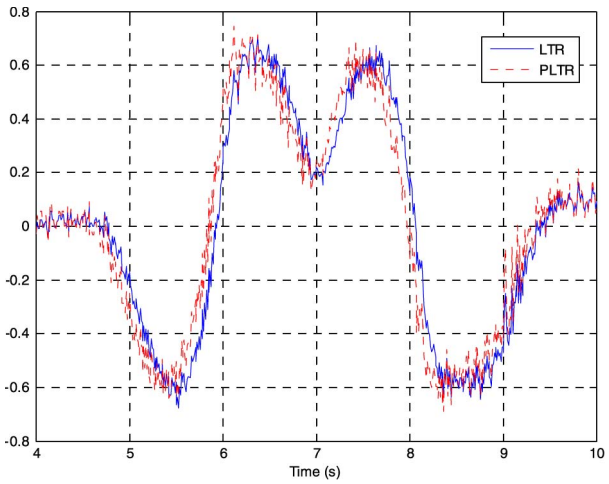

Fig. 9. Double-lane change (experimental measurements).

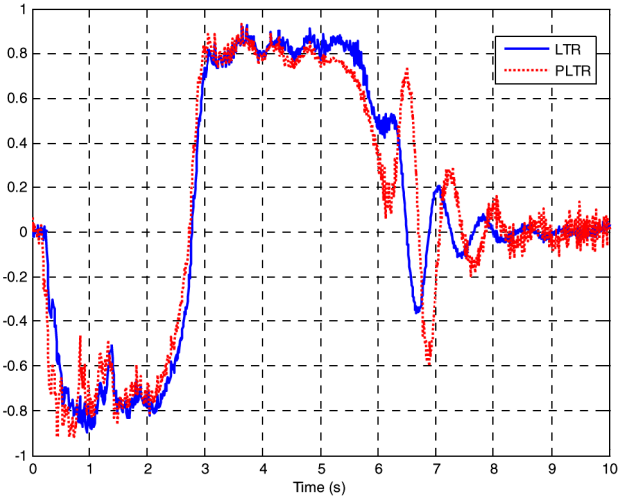

Fig. 10. Fishhook maneuver (experimental measurements).

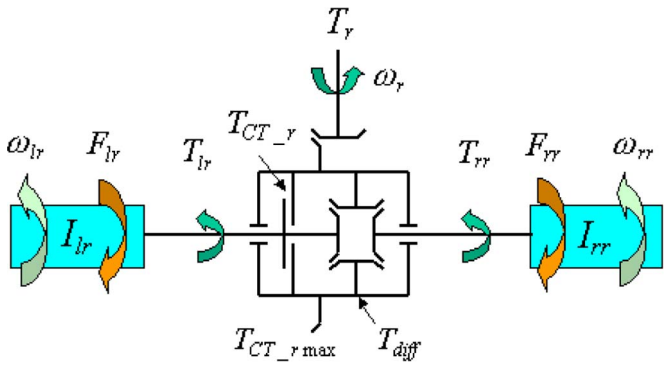

Fig. 11. Electrohydraulically actuated differentials.

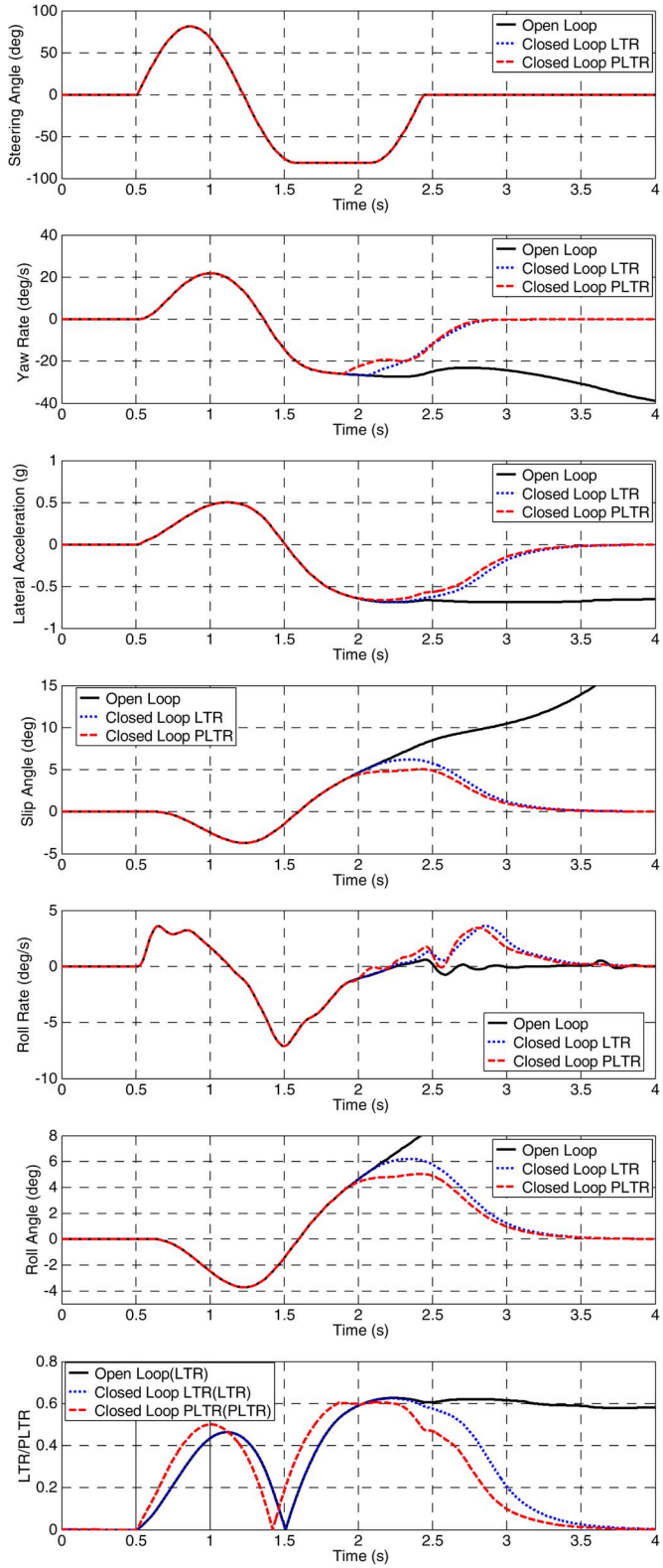

Fig. 12. Simulations. Open- and closed-loop performance comparison for the "Sine with Dwell" maneuver at 81.3° steering amplitude.

Fig. 8 shows the calculated LTR and PLTR from experimental vehicle test data for the "Sine with Dwell" maneuver (open loop). The plots show a good correlation between the simulation study and the actual implementation in the vehicle.

Figs. 9 and 10 further present the calculation of the LTR and the PLTR from experimental vehicle testing data for the North Atlantic Treaty Organization double-lane change maneuver at 90 km/h and a Fishhook maneuver at 64 km/h, respectively. It is also clear from these figures that the PLTR provides a small but important time advance compared with the LTR index. Further, in all of these experimentally validated steering maneuvers, there is a good match in the shape of LTR and PLTR trajectories.

Fig. 13. Test vehicle: Humvee (HMMWV M1152).

V. Closed-Loop Simulation Comparison

This section presents the simulation results acquired from closed-loop simulation in CarSim, utilizing the different rollover indexes studied in this paper. The simulation model includes the vehicle model in CarSim, an active differential driveline configuration modeled in AMESim, and baseline control programs in MATLAB-Simulink. The active differentials are electrohydraulically actuated and have the ability to proportionally operate from fully open to fully locked, thus effectively control the vehicle's yaw and roll motions. A schematic of the differentials is shown in Fig. 11. More details on the active differentials and their influence on vehicle yaw stability and vehicle roll dynamics are available in [15].

The adopted baseline control law is given in (19). When the estimated LTR reaches the value of 0.6, the differentials are engaged 50%, and then, the engagement is proportionally increased to full lock, i.e., 100% engagement, when the LTR reaches a value of 0.8. Thus

$$u = \underset{100}{sat}\left[a \cdot \underset{[0\ 0.6]}{deadzone}\{\text{LTR}\} + b\right] \tag{19}$$

where $(a, b) = (250, -100)$.

The threshold setting in (19), e.g., 0.6, may not be suitable for every maneuver type due to the steady-state nature of the LTR calculation; however, it could be considered a conservative estimate to prevent rollover for normal driving situations. The PLTR is proposed to capture the dynamics of the LTR and address the challenge in setting the threshold for the control law. Hence, the robustness to the maneuver variation can be improved.

To validate the PLTR, a simulation was performed with CarSim to analyze the impact of the new controller compared with a vehicle with the control system off and a vehicle with the LTR active. The performance of the vehicle is compared utilizing the steering angle, yaw rate, lateral acceleration, slip angle, roll rate, and roll angle indexes for the "Sine with Dwell" maneuver at 81.3° amplitude. The control system off (open loop) testing was first completed to establish baseline vehicle dynamics. Fig. 12 shows that as the vehicle in the open-loop case begins the second-turn portion of the maneuver, it becomes unstable, and the roll angle climbs as the vehicle has high susceptibility to roll over. The vehicles with the LTR and the PLTR match well until the midpoint of the second turn when the PLTR system activates prior to the LTR. Both vehicles are able to remain stable throughout the remainder of the maneuver.

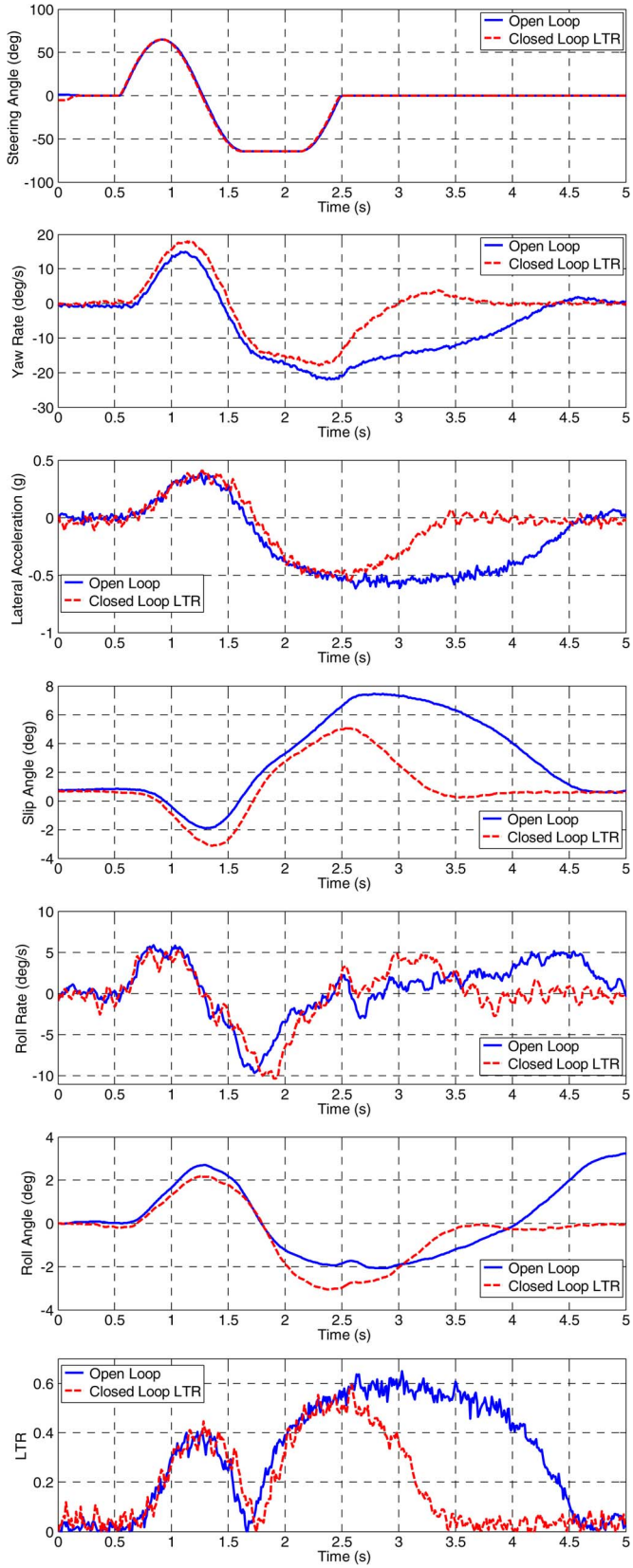

Fig. 14. Experiments. "Sine with Dwell" test results at 65° steering angle sine amplitude.

However, the vehicle with the PLTR manages a 20% reduction in roll angle. This decreases the likelihood of roll over and allows a quicker run time. The superiority of the PLTR can be

further shown in the closed-loop experiments, where the same "Sine with Dwell" maneuver is executed but with significantly larger steering angles.

VI. Closed-Loop Experimental Results

The developed estimation algorithm was validated with experimental measurements on a military test vehicle, i.e., HMMWV M1152 (see Fig. 13). An electronic control unit from Mototron was used for model-based control implementation and a dSpace MicroAutobox was used for data acquisition. A high-fidelity real-time one-antenna Global Positioning System (GPS), i.e., RT3000 with a high-accuracy inertial measurement unit (IMU), from Oxford Technical Solutions, was used to accurately measure vehicle dynamics signals. RT3000 is a full six-axis inertial navigation system with combined GPS. An in-vehicle steering/accelerating robot from Antony Best Dynamics was used to achieve repeatable testing.

The "Sine with Dwell" maneuver was initially performed without closed-loop control (open loop) to determine baseline vehicle dynamics. The vehicle was iteratively tested while increasing the steering amplitude until failure, as specified in the FMVSS126 standard, occurred. Then, the vehicle was tested utilizing the closed-loop LTR and compared with the baseline.

Fig. 14 shows the vehicle characteristics with the control off (open loop) and with the LTR control at an amplitude of 65°. The open-loop vehicle becomes unstable during the first turn and slides through the maneuver as indicated by the yaw angle, lateral acceleration, and slip rate angle values. Comparatively, the vehicle with the LTR control remains stable throughout the maneuver and demonstrates a significant reduction in yaw rate, lateral acceleration, and slip angle. Further, the vehicle exhibits over 20% reduction in peak roll angle in the first turn, greatly reducing the susceptibility of the vehicle to roll over. In further vehicle testing, the LTR controller achieved a stability limit of up to 113.8° in steering amplitude (74% improvement above baseline).

The final testing was performed on the vehicle with the PLTR controller to validate the system and compare the control system performance with respect to the LTR and baseline systems.

Fig. 15 shows the vehicle dynamics associated with the PLTR and the LTR at 130° steering amplitude. The PLTR and LTR dynamics match well in the initial turn and begin to deviate as the PLTR activates for a moment at the end of the first turn. Both control types allow the vehicles to complete the maneuver. However, only the PLTR control is able to satisfy the requirements of the FMVSS126 standard as indicated by the reduced yaw rate after the second turn. Further, the PLTR was able to reduce the roll angle by 14.5% in the second turn, which reduces the propensity to roll over and allows the vehicle to remain on course throughout the maneuver. The open-loop system could not be tested at the 130° amplitude, since it was unstable at this amplitude.

Further experiments were carried out in which the steering angle was increased little by little until yaw instability occurred. The vehicle utilizing the LTR-based closed-loop system was able to achieve a maximum steering angle of 113.8°, whereas

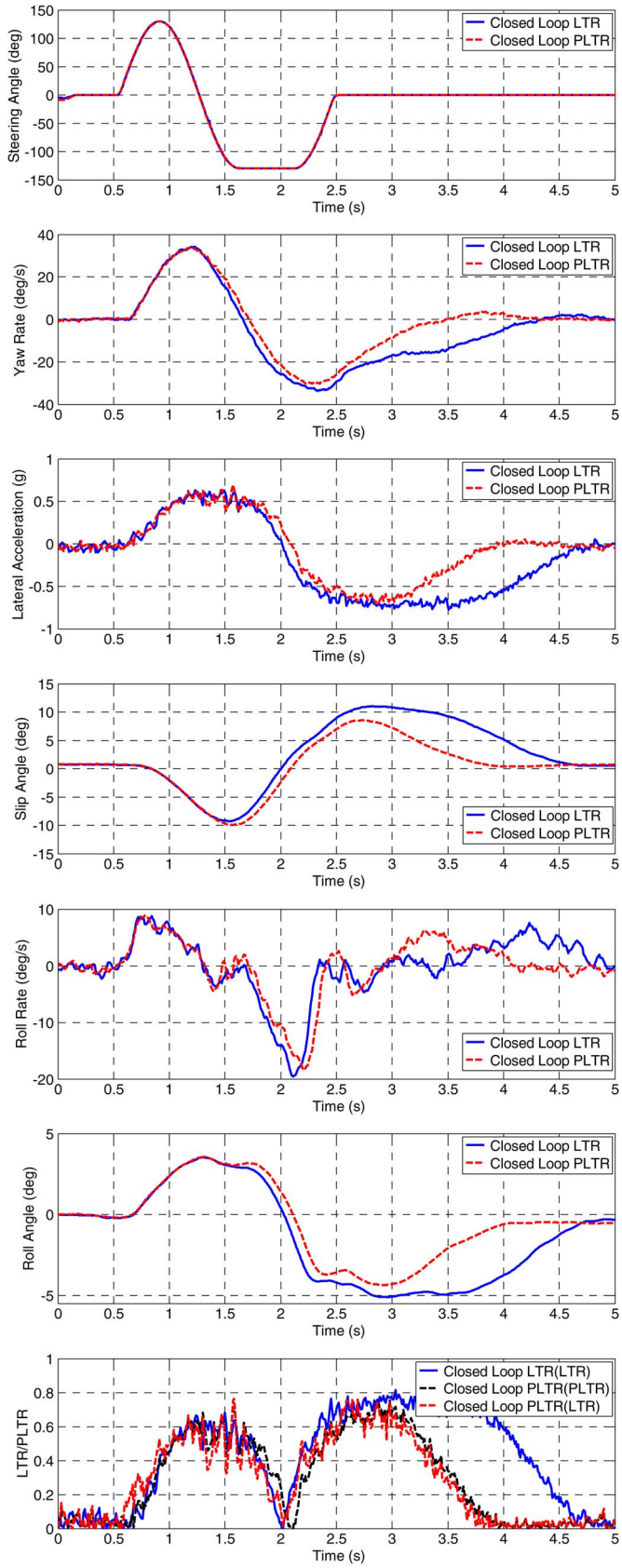

Fig. 15. Experiments. "Sine with Dwell" test results at 130° steering angle sine amplitude.

the vehicle utilizing the PLTR-based control system was able to reach a 162.5° steering angle before it became unstable. This equated to an improvement of 150% above baseline and

43% above LTR. The quantitative value of the improvement is specific to this particular type of roll test.

VII. Conclusion

In this paper, the PLTR index has been proposed for detection of rollover and compared against the commonly used LTR index that utilizes lateral acceleration and roll angle. The PLTR index utilizes steering angle and other sensor signals typically available on all ESC systems. The PLTR is shown to provide a time advance in the detection of rollover threats compared with the LTR index. Simulation results using the industry-standard software CarSim are presented on the comparison of performance using the two indexes. Experimental results using "Sine with Dwell," fishhook and double-lane change steering maneuvers are presented on open-loop index comparison. Closed-loop experiments are presented using the "Sine with Dwell" maneuver. The largest steering amplitude before the onset of yaw instability is computed for the two indexes. It is shown that the closed-loop PLTR system provides superior performance and can handle 43% larger steering angles before instability compared with the LTR system.

References

[1] National Highway Traffic Safety Administration (NHTSA). [Online]. Available: www.nhtsa.dot.gov

[2] L. Xu and H. Eric Tseng, "Robust model-based fault detection for a roll stability control system," *IEEE Trans. Control Syst. Technol.*, vol. 15, no. 3, pp. 519–528, May 2007.

[3] A. Hac, "Rollover stability index including effects of suspension design," presented at the SAE World Congr., Detroit, MI, USA, 2002.

[4] A. Hac, "Influence of active chassis systems on vehicle propensity to maneuver-induced rollovers," presented at the SAE World Congr., Detroit, MI, USA, 2002.

[5] H. Yang and L. Y. Liu, "A robust active suspension controller with rollover prevention," presented at the SAE World Congr., Detroit, MI, USA, 2003.

[6] J. Gertsch and O. Eichelhard, "Simulation of dynamic rollover threshold for heavy trucks," SAE Paper 2003013385, Int. Truck Bus Meeting Exhib., Ft. Worth, TX, USA.

[7] B. Johansson and M. Gafvert, "Untripped SUV rollover detection and prevention," in *Proc. 43rd IEEE Conf. Decis. Control*, Dec. 14–17, 2004, pp. 5461–5466.

[8] D. Odenthal, T. Bunte, and J. Ackermann, "Nonlinear steering and breaking control for vehicle rollover avoidance," in *Proc. Eur. Control Conf.*, Karlsruhe, Germany, 1999.

[9] P. J. Liu, S. Rakheja, and A. K. W. Ahmed, "Detection of dynamic roll instability of heavy vehicles for open-loop rollover control," in *Proc. SAE Int. Truck Bus Meeting*, Cleveland, OH, USA, 1997, pp. 105–112, SAE Paper 973263.

[10] J. Y. Lew, D. Piyabongkarn, and J. A. Grogg, "Minimizing dynamic rollover propensity with electronic limited slip differentials," *SAE Trans. J. Passenger Cars—Mech. Syst.*, pp. 1183–1190, 2007, SAE book number V115-6.

[11] S. Solmaz, M. Akar, R. Shorten, and J. Kalkkuhl, "Realtime multiple-model estimation of center of gravity position in automotive vehicles," *Veh. Syst. Dyn. J.*, vol. 46, no. 9, pp. 763–788, Sep. 2008.

[12] S. Solmaz, M. Corless, and R. Shorten, "A methodology for the design of robust rollover prevention controllers for automotive vehicles with active steering," *Int. J. Control*, vol. 80, no. 11, pp. 1763–1779, Nov. 2007.

[13] D. Piyabongkarn, R. Rajamani, J. A. Grogg, and J. Y. Lew, "Development and experimental evaluation of a slip angle estimation for vehicle stability control," in *Proc. Amer. Control Conf.*, Minneapolis, MN, USA, Jun. 14–16, 2006, pp. 5366–5371.

[14] R. Rajamani, *Vehicle Dynamics and Control,* 2nd ed. New York, NY, USA: Springer-Verlag, 2012.

[15] D. Piyabongkarn, R. Rajamani, J. Y. Lew, and J. A. Grogg, "Active driveline torque management systems—Individual wheel torque control for active automotive safety applications," *IEEE Control Syst. Mag.*, vol. 30, no. 4, pp. 86–102, Aug. 2010.

Chad Larish received the B.S. degree in mechanical engineering from Iowa State University, Ames, IA, USA, in 2009. He is currently working toward the M.S. degree in mechanical engineering with the University of Minnesota, Minneapolis, MN, USA.

He is currently a Senior Systems Engineer with the Advanced Systems Group, Eaton Corporation, Eden Prairie, MN, USA. His research interests include automotive and construction machine propulsion, electrohydraulic control systems, vehicle dynamics, drivetrain control, and energy recovery systems.

Damrongrit (Neng) Piyabongkarn received the B.E. degree from Chulalongkorn University, Bangkok, Thailand; the M.S. degree from the University of Texas at Arlington, TX, USA; and the Ph.D. degree from the University of Minnesota, Minneapolis, MN, USA, all in mechanical engineering.

He is currently a Manager of the Control Systems and Solutions Group, Innovation Center, Eaton Corporation, Eden Prairie, MN, USA. His research interests include advanced controls, system identification, and state estimation, with applications to automotive, hybrid, and electrohydraulic systems and microsensor design.

Dr. Piyabongkarn received the 2007 O. Hugo Schuck Award and the Society of Automotive Engineers 2006 Arch Colwell Merit Award. He received the Doctoral Dissertation Fellowship (2003–2004) from the University of Minnesota.

Vasilios Tsourapas received the M.S. degree in marine engineering from the National Technical University of Athens, Athens, Greece, in 2003 and the M.S. degree in mechanical engineering and the Ph.D. degree in marine engineering from The University of Michigan, Ann Arbor, MI, USA, in 2005 and 2007, respectively.

He is currently an Engineering Specialist with Eaton Corporation, Innovation Center, Eden Prairie, MN, USA. His research interests include optimal controls, system optimization, and power management, with applications to hybrid drivetrain optimization, vehicle dynamics, alternative power generation, and exhaust after-treatment systems.

Dr. Tsourapas received the Department of Defense Graduate Fellowship (2005–2007). His Ph.D. research was funded by the Office of Naval Research, the National Science Foundation, and the Automotive Research Center of The University of Michigan.

Rajesh Rajamani received the M.S. and Ph.D. degrees from the University of California, Berkeley, CA, USA, in 1991 and 1993, respectively, and the B.Tech. degree from the Indian Institute of Technology at Madras, Chennai, India, in 1989.

He is currently a Professor of mechanical engineering with the University of Minnesota, Minneapolis, MN, USA. He has authored over 95 journal papers and is a co-inventor on eight patent applications. He is the author of the popular book *Vehicle Dynamics and Control* (Springer Verlag, New York, NY, USA). His active research interests include sensors and control systems for automotive and biomedical applications.

Dr. Rajamani has served as the Chair of the IEEE Technical Committee on Automotive Control and on editorial boards of the IEEE Transactions on Control Systems Technology and the IEEE/ASME Transactions on Mechatronics. He is a Fellow of the American Society of Mechanical Engineers. He received the CAREER award from the National Science Foundation, the 2001 Outstanding Paper award from the IEEE Transactions on Control Systems Technology, the Ralph Teetor Award from The Society of Automotive Engineers, and the 2007 O. Hugo Schuck Award from the American Automatic Control Council.